Colloid and Polymer Science (2019) 297:107–114
https://doi.org/10.1007/s00396-018-4442-4

ORIGINAL CONTRIBUTION

Synthesis and characterization of SDS assistant α-alumina structures and investigation of the effect of the calcination time on the morphology

Sema Vural[1] · Özlem Sari[2]

Received: 31 July 2018 / Revised: 5 November 2018 / Accepted: 19 November 2018 / Published online: 28 November 2018

Abstract
In this paper, α-alumina structures were successfully prepared via hydrothermal synthesis supported with sodium dodecyl sulfonate anionic surfactant. The effect of the surfactant and the calcination time were investigated. The characterization of the samples calcinated at 1200 °C was performed using Raman spectroscopy, X-Ray Difraction analysis, Fourier transform infrared spectroscopy, thermogravimetric analysis, and scanning electron microscopy techniques. Experimental results showed that pure α-Al_2O_3 structures were obtained with different morphologies.

Keywords Alumina · Sodium dodecyl sulfonate · Hydrothermal synthesis · Morphology · Calcination

Introduction

Alumina (Al_2O_3) is one of the most commonly used inorganic materials in industrial chemistry due to its mechanical, electrical, thermal, and optical properties [1]. As one of the most important materials, it has been used in many applications as a catalyst or a catalyst support, absorbent, or surface coating [2]. It is also used in machine components [3], microelectronics [4], refractories [5], and optics and lasers [6]. Al_2O_3 is a structural complex oxide which has several different metastable phases and eventually converts to thermodynamically stable α-Al_2O_3. Alumina can generally be divided into two large groups according to crystal structures. These are the surface-centered cubic system (FCC) and the hexagonal cubic system (HCP) according to their position in the crystal structure of oxygen anions. The distribution of the cation in the crystal structure causes these subgroups to have many alumina polymorphs. The aluminum forms in the HCP crystal arrangement are shown in the form of chi (χ-), kappa (κ-), and alpha (α-) while gamma (γ-), eta (η-), delta(δ-) forms are shown in the FCC crystal arrangement. The stable single phase of alumina is an alpha form with high thermal stability, chemical resistance, and hardness and is obtained by a calcination processes at 1230 °C [7, 8]. Bohmite structure (AlOOH) is the most preferred starting material in alpha alumina synthesis. In the literature, various temperatures regarding the phase transformation are given but the most accepted temperatures can be shown as: bohmite→ γ (300 °C); γ → δ (850 °C); δ → θ (1100 °C); θ → α (≥ 1200 °C) [9–12].

Traditional processes for synthesizing α-Al_2O_3 involve mechanical milling [13, 14], vapor phase reaction [15, 16], precipitation [17], sol-gel [18], hydrothermal [19], and combustion methods [20]. All these methods have specific limitations. For instance, the precipitation method suffers from its complexity and long washing and aging time. The sol-gel method based on molecular precursors generally makes it necessary to use high-price alkoxides and it needs long gelation periods [21]. Hydrothermal synthesis is one of the most preferred synthetic ways to obtain inorganic oxides because of its ability to synthesize large crystals of high quality.

Chemical methods are simple ways to synthesize various crystals with different properties under moderate conditions which makes them indispensable. In chemical synthesis, particle formation takes place in three steps: nucleation, particle growth, and finishing. The particle growth step which is called Ostwald's ripening is the most significant step in the process which occurs with the combination of the ions in the solution to form larger particles. Reducing the solubility of the growing

✉ Sema Vural
svural@konya.edu.tr; semavural@gmail.com

[1] Seydişehir AC Eng. Fac. Metal. & Materials Eng., Necmettin Erbakan University, 42370 Konya, Turkey

[2] Institute of Science, Necmettin Erbakan University, 42090 Konya, Turkey

particles in solution ends the particle growth [22]. During chemical synthesis, the existence of another substance which will limit the growth step in the reaction medium and which will not make any contribution to the reaction causes the particle size to be limited. For this purpose, the use of various surfactants and coating the particles with polymer, silica, carbon, or metal are widely used methods [23].

Surfactants are added to the precursor solution to delay the growth of crystals and to reduce the agglomeration [24]. Mirjalili et al. prepared ultrafine nano α-Al_2O_3 particles using an aqueous solution of aluminum isopropoxide and aluminum nitrate hydrate. They showed that addition of surfactants such as sodium dodecylbenzene sulfonates and sodium bis-2-ethylhexylsulfosuccinate affected the particle size, the shape of the produced nanoparticles and their degree of aggregation [18]. Zhu et al. synthesized mesopore alumina microfibers using PEG with different molecular weights (Mn = 400–20.000) as template by hydrothermal route. The obtained alumina microfibers have the different high surface area but the nearly same pore diameter about 3.5 nm. The results indicated that complete transformation to α-alumina has done at 1573 K, and the PEG template indeed played a role in the formation of the fiber-like alumina, but the mesopores within the alumina microfibers may be formed with the amorphous alumina framework during gases burning out in the thermal calcination process [25]. More recently, Ghanizadeh et al. reported that alumina seed had no effect on formation of transient alumina phase during hydrothermal treatment ($\leq$ 220 °C) when processing was performed with aluminum chloride, ammonia solution, and TEAH (tetraethyl ammonium hydroxide) in the presence of Tween-80 and ß-alanine [26]. Surfactant supported synthetic routes were mostly used at the sol-gel synthesis of alumina powders in the literature which needs expensive starting materials and long gelation times [27–29]. At the present study, we introduced synthesis of anionic surfactant supported α-Al_2O_3 powders via hydrothermal route.

The aim of this study is the investigation of the α-Al_2O_3 formation in the presence of the anionic surfactant, sodium dodecyl sulfonate (SDS), as a structure directing agent. The effect of the calcination time on the structure is also investigated. The structural characterization was carried out using Raman, XRD, and FTIR spectroscopies. Structural transformation was interpreted supported by TGA analysis. Morphological identification was screened using SEM images. The total surface area of the samples was analyzed via BET absorption analysis.

Experimental

Chemicals

Aluminum nitrate nonahydrate ($Al(NO_3)_3.9H_2O$) was used as the Al source. Sodium dodecyl sulfonate (SDS) was used as an anionic surfactant. Ammonia solution (35%) was the hydrolysing agent. All the other chemicals were used as received from commercial sources without further purification. The starting solutions were prepared using deionized water.

Synthesis

Surfactant assistant alpha alumina (α-Al_2O_3) structures were successfully prepared by using a hydrothermal technique. A precursor solution (0.3 M) was prepared initially by dissolving aluminum nitrate nonahydrate ($Al(NO_3)_3.9H_2O$) in deionized water and stirred at room temperature for an hour. Surfactant solutions were added to the precursor solutions resulting in 1%, 3%, 5%, and 10% SDS/Al^{+3} mixtures, and the mixtures were stirred for another hour in order to get a homogenous solution. The pH value was adjusted to 10 ± 0.1 using 35% ammonia solution and the solutions were transferred to a Teflon-lined autoclave. The reactions were continued at 180 °C for 9 h. After cooling to room temperature, the products were precipitated by centrifuged at a rate of 12,000 rpm and purified by washing with deionized water several times. The obtained products were dried in a vacuum oven overnight at 40 °C. The crude products were calcinated at 1200 °C for 3 and 6 h, and the effects of the calcination time were investigated, as well (Scheme 1). The structural analyses of the obtained samples were studied by Raman and infrared spectroscopy (FTIR). Morphological characterizations were investigated via scanning electron microscopy (SEM). Thermogravimetric analyses were carried out using crude products to demonstrate the existence of surfactants in the structure. The surface area of the powders was measured by using an automated BET gas adsorption analyzer.

Characterization

Structural analysis were studied via a Renishaw Invia Reflex Confocal (× 100 objective) Raman spectrometer with a 1800 lines/mm grating and 532-nm excitation energy at 200-mW laser power. X-ray diffraction analyses

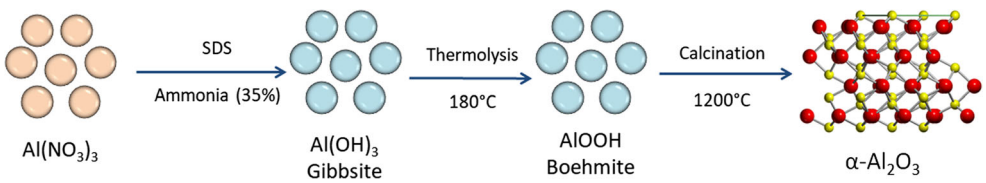

Scheme 1 Schematic illustration of synthesis of the Al_2O_3 powders

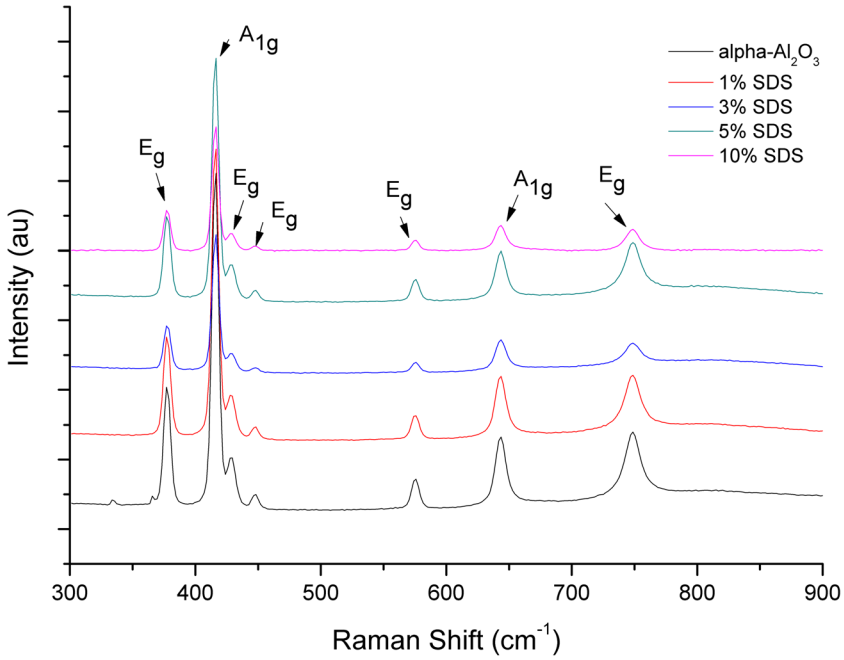

Fig. 1 Raman spectra of prepared Al_2O_3 powders calcined for 6 h

of the samples were performed by using the Rigaku Rad B-Dmax II powder diffractometer. The 2θ values were taken between 20° and 110° using Cu Kα (λ = 1.5405 Å) irradiation in 0.04° steps at a scanning speed of 4°/min. The dried samples were prepared for analysis by spreading 30 (± 2) mg sample into 5 cm^2 area as a thin layer in order to minimize the deviations in the peak values and peak dilatation resulting from the sample thickness. Fourier transform infrared (FTIR) spectra were recorded on an FTIR spectrophotometer equipped with an attenuated total reflectance (ATR) accessory (Nicolet iS5 FTIR) in the range of 550–4000 cm^{-1} in ambient air at room temperature. Thermogravimetric Analysis (TGA) was performed with a Shimadzu TGA-50 thermal analyzer at a heating rate of 10°Cmin¯1 using a 10-mg sample from 30 °C temperature to 900 °C under air atmosphere.

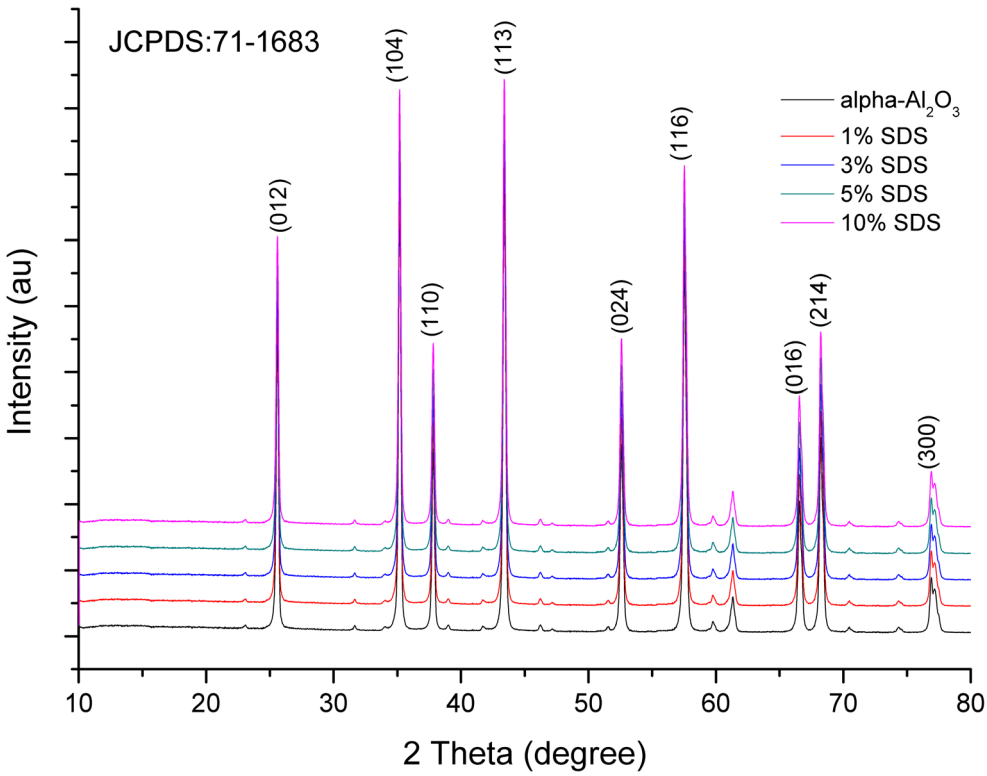

Fig. 2 XRD spectra of prepared α-Al_2O_3 powders calcined for 6 h

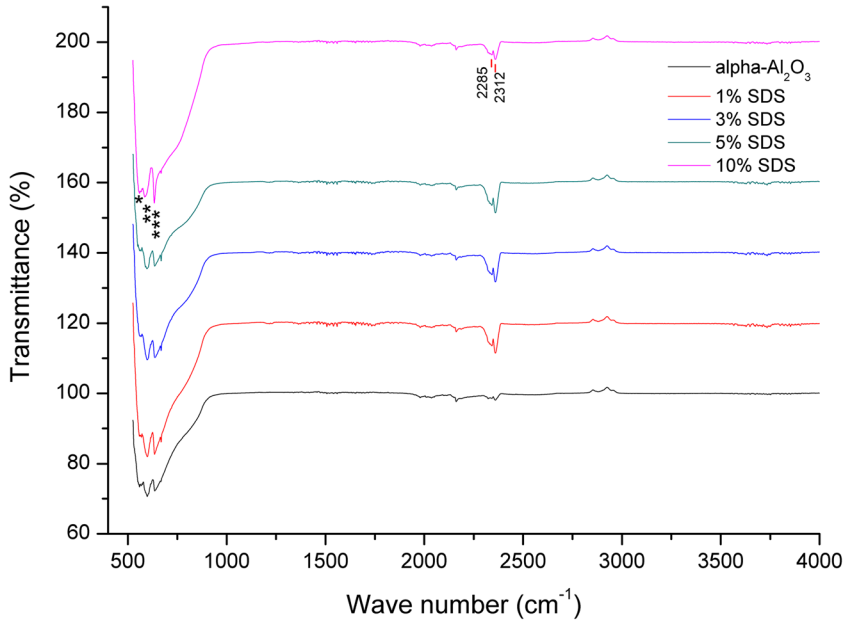

Fig. 3 FTIR spectra of prepared Al_2O_3 powders calcined for 6 h. *549 cm^{-1}, **552 cm^{-1}, and ***631 cm^{-1}

Determination of the morphological properties of the prepared powders was carried out using a Ronteck xflash detector analyzer associated with a scanning electron microscope (Leo-Evo 40XVP). Incident electron beam energies from 3 to 13 keV were used. All samples were sputter coated with Au/Pd before the analyses. The surface area of the alumina samples was measured in a sorption analyzer, Quantachrome Nova, with N_2 as the adsorbed gas, using the Brunauer-Emmett-Teller (BET) method. The BET measurements, nitrogen adsorption-desorption isotherms conducted at 77 K.

Result and discussion

The Raman spectroscopy technique has been extensively used to determine the structure, composition, and phase characterization of the materials. Figure 1 gives the Raman spectra of synthesized α-Al_2O_3 structures. The representation of optical bands in α-Al_2O_3 is given as follows:

$$2A1_g + 2A1_u + 3A2_g + 2A2_u + 5E_g + 4E_u$$

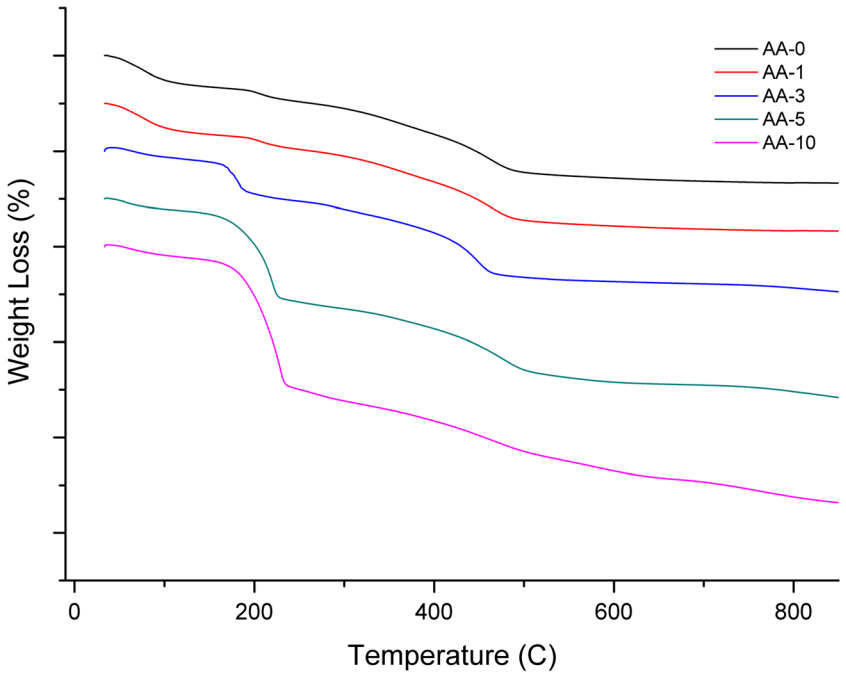

Fig. 4 TGA thermograms of prepared Al_2O_3 powders

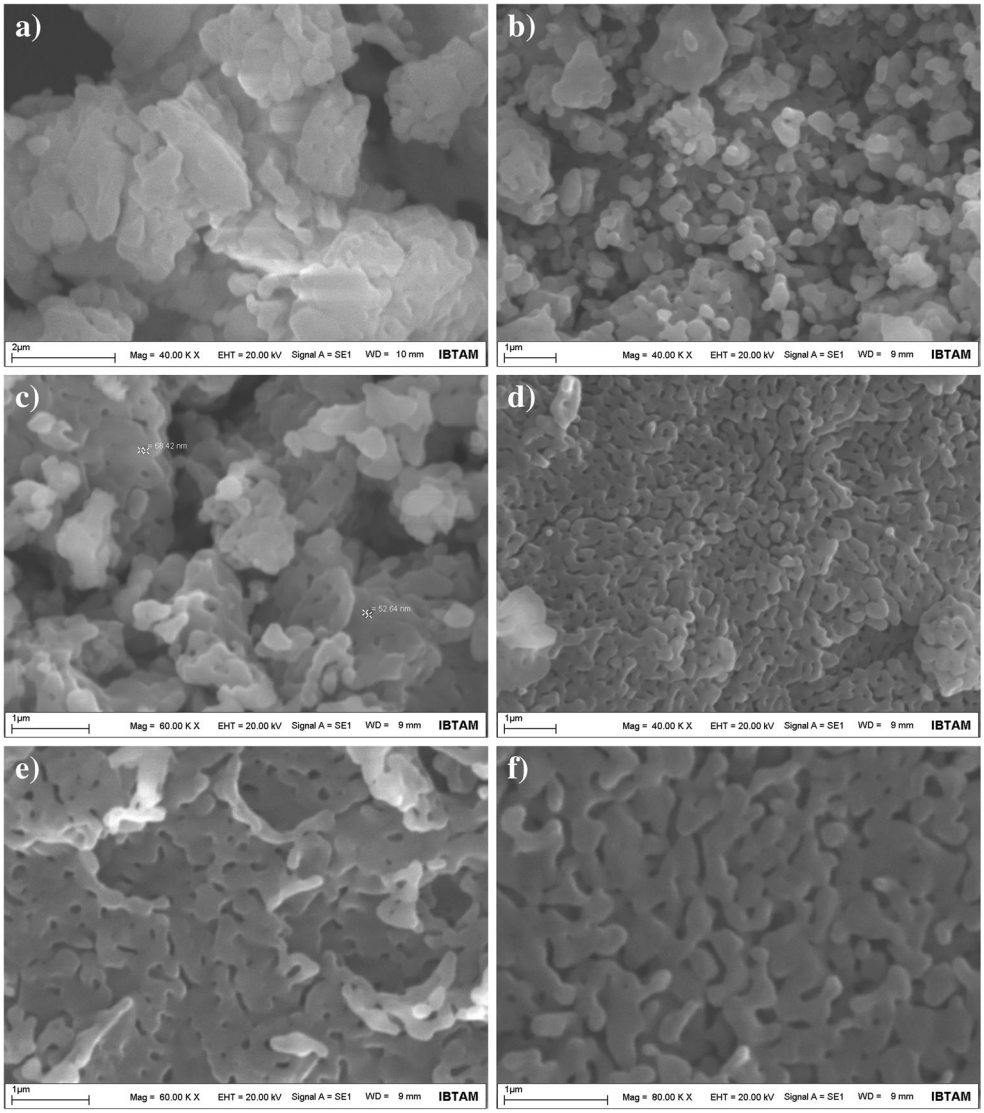

Fig. 5 SEM images of Al_2O_3 powders calcinated at 1200 °C for 6 h. **a** Without surfactant. **b** 1% SDS. **c** 3% SDS. **d** 5% SDS. **e**–**f** 10% SDS additions

where $2A1_g + 5E_g$ are Raman active modes, $2A2_u + 4Eu$ are IR active modes, whereas $2A1_u + 3A2_g$ are neither Raman nor IR active modes. The α-Al_2O_3 gives rise to seven Raman active phonon modes. The Raman bands with peaks at ~378, 431, 453, 581, and 752 cm^{-1} have been assigned to E_g (external), and 416, 645 cm^{-1} peaks have been assigned to $A1_g$ modes [30–32].

XRD results of the synthesized alumina powders calcined at 1200 °C are shown in Fig. 2. The sharp peaks of α-Al_2O_3 at Bragg's angle of 25.58, 35.16, 37.78, 43.36, 52.56, 57.76, 66.52, and 68.20° indicate the relatively large grain sizes and well-defined long-range order in structures [2, 33].

Figure 3 presents the ATR spectra of synthesized Al_2O_3 powders. The bands in the region of 400–1000 cm^{-1} were associated with stretching vibration of Al-O bonds in general. [34] According to the spectra, there are three major peaks shown at 549, 552, and 631 cm^{-1} which are identified to be the characteristic absorption bands of α-Al_2O_3 in octahedral structure [35]. Absorption at 2312 and 2285 cm^{-1} which did not appear at the spectra labeled as α-Al_2O_3, are stretching vibrations of the HCO_3^- group, indicating H_2O and CO_2 absorption in the prepared powders [36]. These peaks also indicate the presence of surfactant in the structure before the calcination.

The TGA analyses were realized using the crude samples Figure 4 shows the alumina precursors which were synthesized using 1% (AA-1), 3% (AA-3), 5% (AA-5), and 10% (AA-10) surfactants and also the precursor in the absence of surfactant (AA-0). According to the thermogram of AA-0 sample, the weight loss up to 250 °C is associated with the solvents which remained inside the sample after drying and water loosely bound. The continuing weight loses after 250 °C can be attributed to the structural rearrangements which occur in regard to –OH group loses resulting from the phase transformation. It is clear that the AA-0 sample is thermally stable after around 550 °C. The thermogram of the AA-1 is very similar to AA-0 at the second stage because there is quite a small amount of surfactant inside the

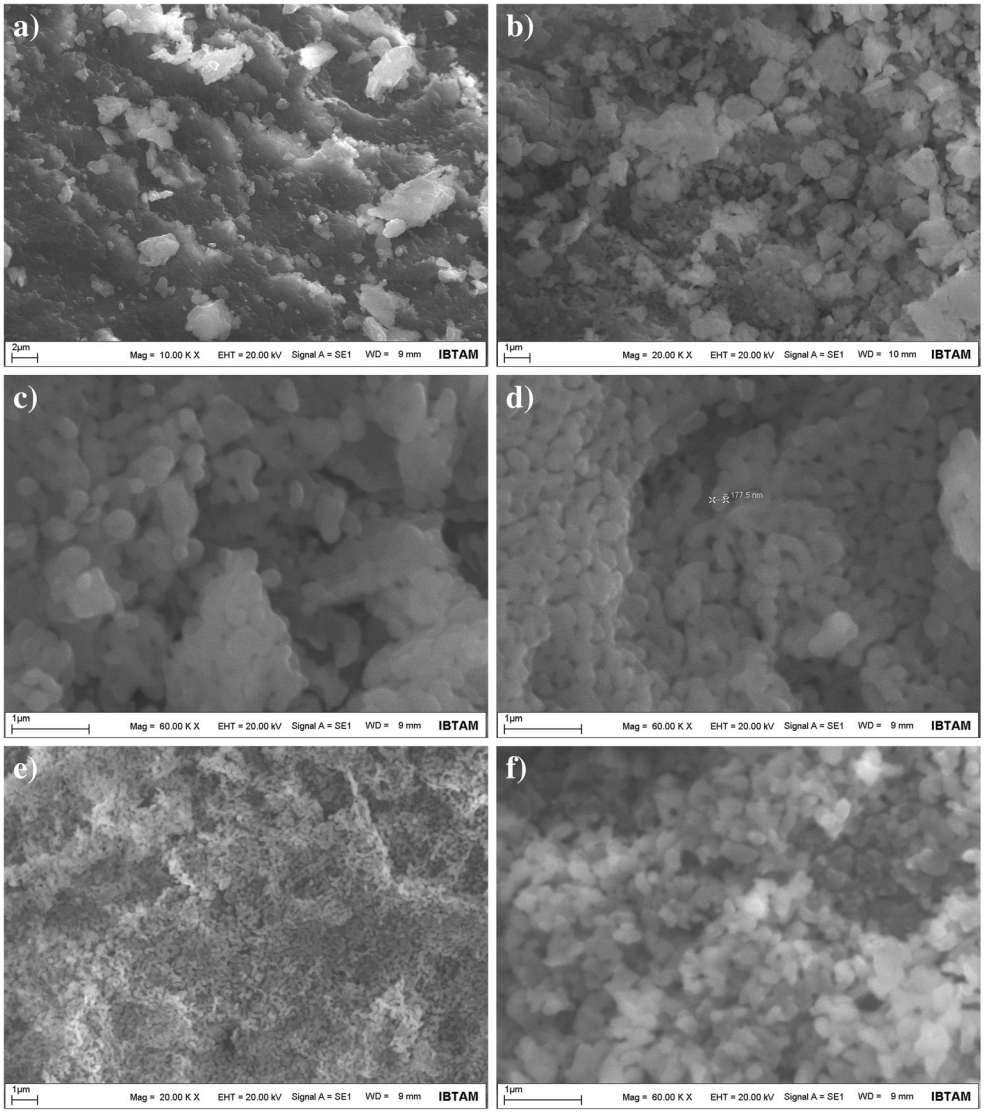

Fig. 6 SEM images of Al_2O_3 powders calcined at 1200 °C for 3 h. **a** Without surfactant. **b** 1% SDS. **c** 3% SDS, **d** 5% SDS. **e**–**f** 10% SDS additions

structure. The weight loss differences become more noticeable as the amount of surfactant increases. The surfactant inside the structure decomposes with the increasing temperature giving decay products of CO_2 and H_2O. This is the reason for the HCO_3^- absorption peak at 2312 and 2285 cm^{-1} in the FTIR spectra. It is reported that the alkyl chain of the surfactant, SDS, was completely removed below 200 °C, where the sulfate head group was lost in the region between 400 and 600 °C [37]. The weight loss at the second stage may be caused not only by the removal of the head group of the surfactant but also by the loss of water in the alumina framework. While the temperature increases the alumina dehydrate to a transitional phase and further to Al_2O_3 [38]. The weight loss continues at the range of analyzing temperature for all surfactant containing samples, and decomposition of the surfactant affects the morphological structure of the samples, as well.

Figure 5 shows the SEM images of calcinated samples which are labeled at the up right corner of each image. It is clear from Fig. 5a that the alumina synthesized in the absence of surfactant appears as a bulk structure. After the addition of 1% SDS to the reaction medium, the resultant structure slightly changes (Fig. 5b). The morphology of the structures dramatically changes with the increasing amount of SDS in the reaction medium (Fig. 5c–d) and it becomes a porous structure when the SDS addition

Table 1 Total surface area of alumina powders at different calcination time

Total surface area (m^2/g)	α-Al_2O_3	1% SDS	3% SDS	5% SDS	10% SDS
3-h calcination	5.073	6.316	7.65	9.509	11.663
6-h calcination	4.73	5.12	5.23	5.43	5.873

increases to 10% (Fig. 5e–f). According to the investigation of Sicard et al. [39], a strong interaction exists between the sulfate head groups and the alumina framework. Sintering likely occurs because the polar surfactant head group strongly interacts with the positive charges of the alumina surface and most likely embedded into the alumina walls. The further removals caused a ready sintering and collapse of the alumina framework upon surfactant removal by calcination which leads to a porous structure [38, 39].

The calcination time also apparently changes the morphology of the synthesized alumina structures. Figure 6 provides the morphology of the structures calcinated at 1200 °C for 3 h. The alumina framework does not have enough time to collapse, and the resultant structures show worm-like morphology after 3-h calcination.

Total surface area of the samples is given at Table 1. It can be seen that with increasing surfactant content, the surface area of the sample increases. However, when calcination time increases to 6 h at the same calcination temperature, the total surface area nearly does not change because of the collapse of the alumina framework. These results are compatible with the SEM images.

Conclusion

α-Alumina structures were synthesized in the presence of the anionic SDS surfactant. The crude samples were calcinated at 1200 °C in air. The SDS molecules strongly interact with the positive charges of the alumina surface and because of these strong interactions, the surfactant head groups remain in the structure at high temperatures. The further removals cause a collapse of the alumina framework upon surfactant removal by calcination which leads to a porous bulk structure. The calcination time affects the morphology of the structures, as well. The structures show worm-like morphology when the calcination time decreases to 3 h. Phase transformation needs high temperature calcinations and a relatively long calcination time. However, increasing calcination time at 1200 °C provides the structure enough time to collapse with the effect of the high temperature, and the resulting structure becomes collapsed bulky material with nano-sized cavities.

Funding information This work is financially supported by the Necmettin Erbakan University Research Fund (Project No: BAP-181331002).

Compliance with ethical standards

Conflict of interest The authors declare that they have no conflict of interest.

References

1. Chandradass J, Yoon JH, Bae D-s (2008) Synthesis and characterization of zirconia doped alumina nanopowder by citrate–nitrate process. Mater Sci Eng A 473:360–364
2. Sun Z-X, Zheng T-T, Bo Q-B, Du M, Forsling W (2008) Effects of calcination temperature on the pore size and wall crystalline structure of mesoporous alumina. J Colloid Interface Sci 319: 247–251
3. Hotta M, Kondo N, Kita H, Ohji T, Izutsu Y, Arima T, Matsumura Y (2015) Joining of alumina with an alumina–zirconia insert under low mechanical pressure. J Asian Ceramic Soc 3(1):59–63
4. Zhoua W, Niu X, Min G, Song Z, Zhang J, Liua Y, Li X, Zhang J, Feng S (2009) Porous alumina nano-membranes: Soft replica molding for large area UV-nanoimprint lithography. Microelectron Eng 86(12):2375–2380
5. Yang J-Z, Fang M-H, Huang Zo-H, Hu X-Z, Liu Y-G, Sun H-R, Huang J-T, Li X-C (2012) Solid particle impact erosion of alumina-based refractories at elevated temperatures. J Eur Ceram Soc 32(2): 283–289
6. Kir'yanov AV, Siddiki SH, Barmenkov YO, Das S, Dutta D, Dhar A, Khakhalin AV, Sholokhov EM, Il'ichev NN, Didenko SI, Paul MC (2017) Hafnia-yttria-alumina-silica based optical fibers with diminished mid-IR (> 2 μm) loss. Opt Mater Express 7(7):2511–2518
7. Levin I, Brandon D (1998). J Am Ceram Soc 81:1995–2012
8. Ravanchi MT, Fard MR, Fadaeerayeni S, Yaripour F (2015) Effect of calcination conditions on crystalline structure and pore size distribution for a mesoporous alumina. J Chem Eng Commun 202(4): 493–499
9. Dwivedi RK, Gowda G (1985) Thermal stability of aluminium oxides prepared from gel. J Mater Sci Lett 4:331–334
10. Saraswati V, Rao GVN, Rao GVR (1987) Structural evolution in alumina gel. J Mater Sci 22:2529–2534
11. Assih T, Ayral A, Abenoza M, Phalippou J (1988) Raman study of alumina gels. J Mater Sci 23:3326–3331
12. Ozao R, Ochiai M, Yoshida H, Ichimura Y, Inada T, Therm J (2001). Anal Calorim 64:923–932
13. Reid CB, Forrester JS, Goodshaw HJ, Kisi EH, Suaning GJ (2008) A study in the mechanical milling of alumina powder. Ceram Int 34(6):1551–1556
14. Forrester JS, Goodshaw HJ, Kisi EH, Suaning GJ, Zobec JS (2008). J Aust Ceram Soc 44(1):47–52
15. Chou TC, Nieh TG (1991) Nucleation and concurrent anomalous grain growth of alpha-Al2O3 during gamma - alpha phase transformation. J Am Ceram Soc 74(9):2270–2279
16. Varma HK, Mani TV, Damodran AD (1994) Characteristics of alumina powders prepared by spray-drying of boehmite sol. J Am Ceram Soc 77(6):1597–1600
17. Lafficher R, Digne M, Salvatori F, Boualleg M, Colson D, Puel F (2017) Development of new alumina precipitation routes for catalysis applications. J Cryst Growth 468:526–530
18. Mirjalili F, Hasmaliza M, Abdullah LC (2010) Size-controlled synthesis of nano α-alumina particles through the sol–gel method. Ceram Int 36:1253–1257
19. Panda PK, Jaleel VA, Usha Devi S (2006) Hydrothermal synthesis of boehmite and α-alumina from Bayer's alumina trihydrate. J Mater Sci 41(24):8386–8389
20. Bhaduri S, Zhou E, Bhaduri SB (1996) Auto ignition processing of nanocrystalline α-Al2O3. Nanostruct Mater 7(5):487–496
21. Li J, Pan Y, Xiang C, Ge Q, Guo J (2006) Low temperature synthesis of ultrafine α-Al2O3 powder by a simple aqueous sol–gel process. Ceram Int 32:587–591

22. Vural S (2007) Formation of nanometric metal oxide sols, structural control and physicochemical characterization. Masters Dissertation, Inonu University
23. Lu AH, Salabas EL, Schüth F (2007) Magnetic nanoparticles: synthesis, protection, functionalization, and zpplication. Angew Chem Int Ed 46:1222–1244
24. Behera PS, Sarkar R, Bhattacharyya S (2016) Nano alumina: a review of the powder synthesis method. Interceram-International Ceramic Review 65(1–2):10–16
25. Zhu Z, Liu H, Sun H, Yang D (2009) Surfactant assisted hydrothermal and thermal decomposition synthesis of alumina microfibers with mesoporous structure. Chem Eng J 155:925–930
26. Ghanizadeh S, Bao X, Vaidhyanathan B, Binner J (2014) Synthesis of nano α-alumina powders using hydrothermal and precipitation routes: a comparative study. Ceram Int 40:1311–1319
27. Khazaei A, Nazari S, Karimi G, Ghaderi E, Moradian KM, Bagherpor Z, Nazari S (2016). Int J Nanosci Nanotechnol 12(4):207–214
28. Tabesh S, Davar F, Loghman-Estarki MR (2018) Preparation of γ-Al2O3 nanoparticles using modified sol-gel method and its use for the adsorption of lead and cadmium ions. J Alloys Compd 730: 441–449
29. Aguado J, Escola JM, Castro MC, Paredes B (2005) Sol–gel synthesis of mesostructured γ-alumina templated by cationic surfactants. Microporous Mesoporous Mater 83(1–3):181–192
30. Cava S, Tebcherani SM, Souza IA, Pianaro SA, Paskocimas CA, Longo E, Varela JA (2007) Structural characterization of phase transition of Al2O3 nanopowders obtained by polymeric precursor method. Mater Chem Phys 103(55):394–399
31. Gangwar J, Gupta BK, Tripathi SK, Srivastav AK (2015) Phase dependent thermal and spectroscopic responses of Al2O3nanostructures with different morphogenesis. Nanoscale 7:13313–13344
32. Pezzotti G, Zhua W (2015) Resolving stress tensor components in space from polarized Raman spectra: polycrystalline alumina. Phys Chem Chem Phys 17:2608–2627
33. Bawa SG, Ahmed AS, Okonkwo PC (2017). Nig J Technol 36(3): 822–828
34. Zhou SX, Antonietti M, Niederberger M (2007) Low-temperature synthesis of γ-alumina nanocrystals from aluminum acetylacetonate in nonaqueous media. Small 3:763–767
35. Djebaili K, Mekhalif Z, Boumaza A, Djelloul A (2015) J Spectro Article ID 868109. 16 pages. https://doi.org/10.1155/2015/868109
36. Sicard L, Llewellyn PL, Patarin J, Kolenda F (2001) Investigation of the mechanism of the surfactant removal from a mesoporous alumina prepared in the presence of sodium dodecylsulfate. Micro Meso Mater 44-45:195–201
37. Qu L, He C, Yang Y, He Y, Liu Z (2005) Hydrothermal synthesis of alumina nanotubes templated by anionic surfactant. Mater Lett 59: 4034–4037
38. Márquez-Alvarez C, Žilková N, Pérez-Pariente J (2008) Synthesis, characterization and catalytic aqpplications of organized mesoporous aluminas. Catal Rev Sci Eng 50(2):222–286
39. Valange S, Guth J-L, Kolenda F, Lacombe S, Gabelica Z (2000). Microporous Mesoporous Mater 35–36:597–607